

# Intelligent Load Frequency Control considering Large Scale Photovoltaic Generation

Awan Uji Krismanto and Herlambang Setiadi

**Abstract**—Large-scale renewable energy integration involving large scale PV plant is becoming popular in the last decade due to global warming and climate change. PV plant offers clean and environmentally friendly electricity. However, PV plant also provides unwanted impact in term of frequency stability. Hence appropriate, load frequency control due to the integration of PV plant is inevitable. This paper proposed an intelligent approach based on a differential evolutional algorithm (DEA) to optimize the control parameters of load frequency control (LFC) device. Time domain simulation was carried out to analyses, the frequency nadir of the system. The simulation results suggested that a significant enhancement of system dynamic behavior was monitored when the control parameters of LFC were optimized using the proposed DEA. Moreover, the proposed algorithm provided a promising result to improve system dynamic response in the system with high penetration of PV power plant.

**Index Term**— Load frequency control, pv plant, differential evolution algorithm.

## I. INTRODUCTION

RENEWABLE energy (RE) based power generation has been increasing significantly in recent year due to its technical, economical and enviromenal benefits. Moreover, fast development of power electronic and energy storage devices have also encouraged implementation of those renewable power generation. As the installed capacities of these novel type of power generations are contiuously growing, it may affect power system operation, planning and control. Specifically, the dynamic behaviour of a power system with high penetrations of RE based power generation would be different to the conventional power system. To provide a good quality of electricity service, voltage and system frequency have to be maintained within its allowable limits. One of the critial concerns in integrating large scale RE power plant is how to maintain system frequency under various circumstances.

Manuscript recieved October 1, 2017; revised November 12, 2017 and March 20, 2018; accepted April 5, 2018.

Awan Uji Krimanto is pursuing his doctoral program with the School of Information and Electrical Engineering, The University of Queensland, Brisbane, Queensland, Astralia (e-mail: a.krismanto@uq.edu.au), Department of Electrical Engineering, National Institute of Technology, Malang, Indonesia (awan\_uji\_krismanto@scholar.itn.ac.id)

Herlambang Setiadi is with School of Information and Electrical Engineering, The University of Queensland, Brisbane, Queensland, Astralia, (e-mail: h.setiadi@uq.edu.au)

With the integration of large scale RE power generation unit, large fluctuation of system frequency potentially occurred due to intermittency and unertainty of RE resources and changing of load conditions. Hence, an equilibrium operating point might be perturbed frequently, resulting in a fluctuation of system frequency and unstable operating conditions [1]. When the power system is subjected to a disturbance, a continous growth of oscillatory condition might happen if the balance condition cannot be resolved, bringing the power system into an unstable situation. In the case of losing a portion of generating power or sudden increase of load, the fluctuation of system frequency emerged, leading to cascaded load shedding or even resulting in partial shut-down or complete black-out.

A frequency problem is usually handled by a load frequency control (LFC) device. The LFC is a part of the automatic generation control (AGC) system which is responsible for providing damping and maintaining frequency stability [2]. However, a severe frequency instability problem might arise when the LFC capacity is not enough to compensate unbalance of generation and demand.

The LFC is a critical device to maintain system frequency. It should be able to provide a fast response to compensate frequency deviation under fluctuation and perturbed circumstances. Many control algorithms have been proposed to ensure robust operation of LFC devices. A conventional PI controller has been widely implemented in LFC control area. However, since the tuning procedure of the PI controller mostly using a trial and error method, it is difficult to find the optimum setting to establish a good system dynamic performance. Another conventional tuning approaches such as modulus optimum criteria and point estimate method require a lot of efforts and time when it is applied for a wide range interconnected power system. Moreover, with the increasing penetration of RE based power plant, the tuning problems become more complicated. Since the tuning procedure should consider the controller of those novel power generation units.

To overcome those concerns, a novel optimization method approach based on differential evolution algorithm (DEA) is proposed. Compare with other evlutionary algorithm, DEA uses a different procedure for mutation and recombination phases and has a minimum number of control parameters which offers more efficient iterative process and faster for converging [3]. Moreover, it allows optimization of fitness function of discrete variables [4].

This paper addresses a tuning procedure of LFC using DEA in a power system environment with penetration of large-scale PV generations. It is expected that the proposed tuning procedure of LFC can enhance the system dynamic response.

Hence, eventually it can improve the dynamic behavior of the power system which incorporated large-scale PV generation. The remainder of the paper is given as follows. Section II represents modelling procedures of the LFC, governor and power system components involving synchronous generator and PV power plant. In section III, optimization procedure based on a differential evolution algorithm is presented. The comparisons of system dynamic responses using three different control approaches and the simulations results are given in section IV. At the end of the paper, the conclusions of the presented works are presented in section V.

## II. SYSTEM MODELING

The following section represents modeling approach of LFC device and power system components. The developed models are then applied in the selected test system to investigate the frequency stability problem in the system with high PV penetration. Moreover, the DEA algorithm is also implemented to optimize the control parameters of the LFC in order to enhance system dynamic responses.

### A. Load Frequency Control

It is obvious in power system operation that the change of electric power affects the system frequency. When the load increases, the system frequency drops due to a lack of generated power from the generator. Conversely, when the generated power is larger than the load, frequency increases due to the surplus of generated power from the generator. To restore the system frequency, the additional power from generation unit should be increased or decreased proportionally to obtain a balance condition between generation and load demand.

As previously mentioned, load fluctuation might cause the fluctuation of frequency. When the frequency fluctuation is not resolved, it will lead to oscillatory condition on frequency. Therefore, it is necessary to have a good method to maintain system frequency. In a conventional power system, regulation of system frequency is facilitated by load frequency control (LFC) device as depicted in Fig.1. It is shown that the generator output in the form of the frequency being detected by the frequency sensor, then the signal will flow toward the LFC block. The LFC block also receives power flow signals between areas of an interconnected power system. Moreover, the LFC provides a signal to control valve of the steam governor that regulates the turbine [5].

The relationship between the turbine and generator rotation can be described using (1)

$$(T_B - T_G) = H \times \frac{d\omega}{dt} \quad (1)$$

where  $T_G$  and  $T_B$  are generator and load couplings respectively. While  $H$  and  $\omega$  are inertia and rotor speed of the generator respectively. Frequency increases if the active power generated by the generator is greater than the required active power. On the other hand, the frequency drops if the active power generated by the generator is less than the demand.

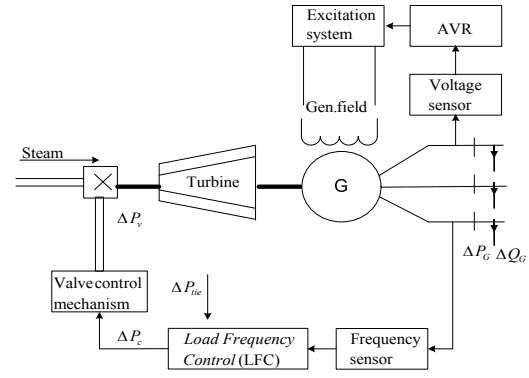


Fig. 1. Schematic diagram of LFC

Active power generator arrangement is made by adjusting the coupling drive the generator. Therefore, controlling system frequency can be realized by regulating the prime movers. The mathematical representation of increasing and decreasing frequency stated in (2) and (3).

$$T_G - T_B = \Delta T < 0, \text{ so } d\omega/dt < 0, \text{ frequency decrease} \quad (2)$$

$$T_G - T_B = \Delta T > 0, \text{ so } d\omega/dt > 0, \text{ frequency increase} \quad (3)$$

### B. System Modeling

For simplicity, the dynamic of a synchronous generator can be represented using the swing equation. For small disturbance, the swing equation of the synchronous machine is given by (4) [6].

$$\frac{2H}{\omega_s} \frac{\partial^2 \Delta\delta}{\partial t^2} = \Delta P_m - \Delta P_e \quad (4)$$

where  $H$  represents the inertia constant of the synchronous generator. Mechanical active and electrical active power is represented by  $P_m$  and  $P_e$  respectively.

The swing equation can also be represented using small changing in rotor speed as given by (5).

$$\frac{\partial \Delta \frac{\omega}{\omega_s}}{\partial t} = \frac{1}{2H} (\Delta P_m - \Delta P_e) \quad (5)$$

In a per-unit system, equation (5) can be presented as given in (6).

$$\frac{\partial \Delta \omega}{\partial t} = \frac{1}{2H} (\Delta P_m - \Delta P_e) \quad (6)$$

Then equation (6) should be transformed into the Laplace domain as shown in (7).

$$\Delta \Omega(s) = \frac{1}{2H} [\Delta P_m(s) - \Delta P_e(s)] \quad (7)$$

From Eq. (7), a block diagram of generator rotor speed is presented in Fig. 2.

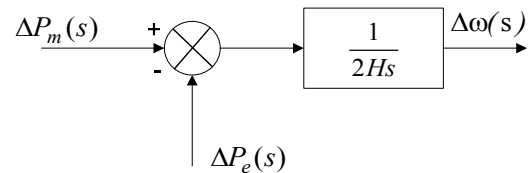


Fig. 2. Block diagram of the generator [6].

Loads in power system comprised of a variety of electrical equipment. A static load such as lamps and electric heater are not influenced by the frequency oscillation. Conversely, the dynamic load such as an electric motor is very sensitive to frequency fluctuation. Therefore, a load fluctuation can be represented as a function of active power and system frequency. The change of active power under a load fluctuation event can be started using (8).

$$\Delta P_e = \Delta P_L + D\Delta\omega \quad (8)$$

Where  $\Delta P_L$  and  $D$  represent load changing and damping constant respectively. Equation (8) can be transformed into block diagram as depicted in Fig. 3.

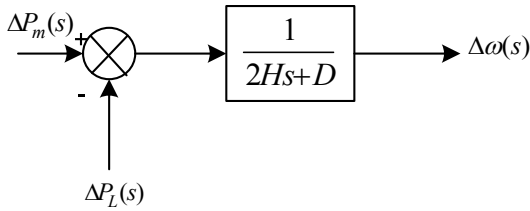
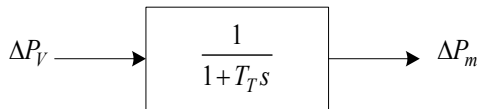


Fig. 3. Block diagram of generator considering load changing [6].

The source of mechanical energy is called a prime mover which can be powered by water, gas, and steam. In this research, the prime movers model is non-reheat steam prime movers or can be called as a non-reheat steam turbine. Turbine model is related to mechanical power output ( $P_m$ ) and the position of the steam valve ( $P_V$ ). Steam turbine model can be approximated by a simple time constant as stated in (9). Equation (9) can be transformed into a block diagram as shown in Fig. 4.

$$G_T = \frac{\Delta P_m(s)}{\Delta P_V(s)} = \frac{1}{1 + T_T s} \quad (9)$$



Fi. 4. Block diagram of a turbine [6].

As previously mentioned, the load fluctuation affects the system frequency. Therefore, to maintain system frequency under the load change, a governor is introduced. When the load on the generator increases suddenly, the mechanical power exceeds the electrical power. This resulted in reduced kinetic energy, causing the speed of the turbine and the frequency of generator drops. The governor detects this speed fluctuation. Governor in charge of giving the action against the inlet valve of the prime movers for change the mechanical output power to bring turbine speed in a stable condition. Under a stable operation, the governors are designed to constrain the speed reduction of the expense increase of active power. Steady-state characteristics of the governor are shown in Fig. 5.

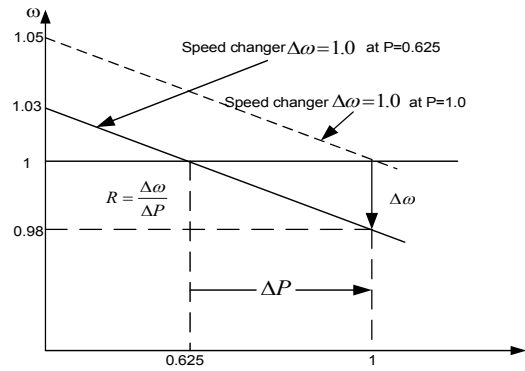


Fig. 5. Steady-state characteristic of the governor [6].

The slope of the governor has a special provision which is 5 to 6 percent of zero until finding the best condition. The speed governor mechanism work as a comparator to the output of the governor ( $\Delta P_G$ ). It consists of the power reference ( $\Delta P_{ref}$ ) and governor characteristic ( $\frac{1}{R}\Delta\omega$ ). This can be described using (10).

$$\Delta P_G = \Delta P_{ref} - \frac{1}{R}\Delta\omega \quad (10)$$

Transform Eq. (10) into Laplace domain as state in (11) [4].

$$\Delta P_G(s) = \Delta P_{ref}(s) - \frac{1}{R}\Delta\Omega(s) \quad (11)$$

The  $\Delta P_G$  transformed into hydraulic reinforcement as a steam valve position command ( $\Delta P_V$ ). The assumed relationship is a linear system and considers the time delay of the governor ( $T_G$ ), then the equation in the Laplace domain can be described using (12). Fig. 6 depicts the block diagram representation of Eq. (12).

$$\Delta P_V(s) = \frac{1}{1 + T_G s} \Delta P_G(s) \quad (12)$$

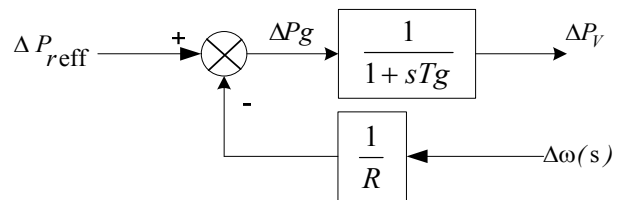


Fig. 6. Block diagram of the governor [6].

By combining the block diagram of the generator with load, turbine, and governor, isolated LFC can be obtained as depicted in Fig. 7 [6].

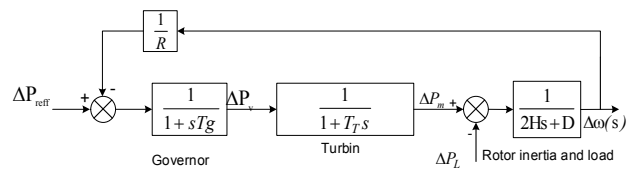


Fig. 7. Isolated LFC [6].

### C. PV Plant Model

PV plant model comprises of three important parts; PV array, power electronics devices, and the associated controller. PV array output current can be described using (13) [7], [8].

$$I_{PV} = I_{SCA}(G) - N_p I_0 \left[ \exp \frac{(V_A + I_{PV} R_s) q}{n N_s k T} - 1 \right] \quad (13)$$

Where  $k$  = Boltzmann's constant ( $1.38e^{-19}$ ),  $T$  = temperature (K),  $I_{PV}$  = array current (A),  $V_A$  = array voltage (V),  $q$  = charge of an electron ( $1.6e^{-19}$  C),  $n$  = ideality factor,  $I_0$  = reverse saturation current of diode (A),  $R_s$  = array series resistance (ohm),  $I_{SCA}(G) = N_p I_{SC}(G)$ ,  $I_{SC}$  = cell short-circuit current (A),  $G$  = solar insolation ( $W/m^2$ ),  $N_p$  = number of modules in parallel;  $N_s = N_{CS} N_{SM}$ ,  $N_{CS}$  = number of series connected cells in a module, and  $N_{SM}$  = number of modules in series.

For load frequency study, PV generation modeled into a set of two-order differential equation [8]. Fig. 8 shows the block diagram of the PV generation for LFC study.

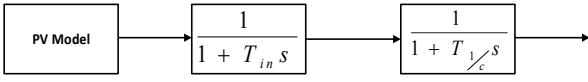


Fig. 8. PV model [9].

### D. PID controller

Stability of the system cannot be separated from their errors caused by small or large perturbation. This error can cause fluctuation in the dynamic behaviors of the system and lead to the unstable condition. Hence, to reduce the system errors and maintain the stability of the system, a controller is inevitable devices in the system. Among the number of the controller, the PID controller is the most employed devices in among industry practitioners. PID controller provides fast response and easy to use [5], [10], [11]. PID controller also accelerates the reaction of the system, eliminating offset and produce large initial changes. Fig. 9 shows the block diagram of a PID controller.

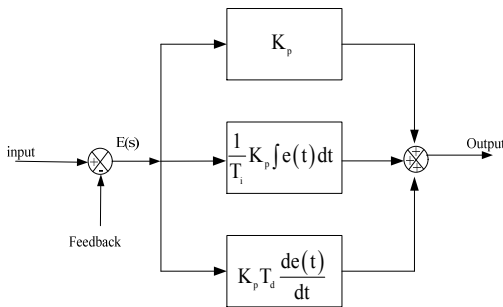


Fig. 9. Block diagram of PID controller [5], [10], [11].

## III. DIFFERENTIAL EVOLUTION ALGORITHM

In general, the optimization technique must qualify to handle the cost function that is non-differentiable, nonlinear and multimodal and has a good convergence. Differential evolution algorithm (DEA) is one method of finding the optimum value which has been designed to meet these requirements. This method was introduced by Storn and Prince [12]–[14] initialization initial value DEA randomized in a particular area that has a limitation. The limit is comprised of an upper limit (**bu**), and the lower limit (**bl**) determined for each parameter.

The value of each initial vector generated randomly between these limits. The mathematical representation of initializing the population is stated in (14).

$$x_{j,i,g} = \text{rand}_j(0,1) \times (b_{j,U} - b_{j,L}) + b_{j,L} \quad (14)$$

After initialization, the next steps is mutation and recombination to produce a trial vector  $N_p$ . Mutation in DEA called differential mutation; this is done by combining the difference vector of the three randomly vectors to produce a mutant vector. This process can be described using (15).

$$v_{i,g} = x_{r0} + F(x_{r1,g} - x_{r2,g}) \quad (15)$$

With  $v_{i,g}$  and  $F$  are mutant vectors and real number with a range 0-1 respectively. While  $x_{r1}$ ,  $x_{r2}$ , and  $x_{r0}$  are random vectors respectively.

DEA crossover used to supplement the search of differential mutation. The purpose of the crossover is formed trial vector DEA from the parameter values that duplicated from two different vectors, namely the initial vector with the mutant vector. The crossover step can be described using (16).

$$u_{i,g} = u_{j,i,g} = \begin{cases} v_{j,i,g} & \text{if } (\text{rand}_j(0,1) \leq C_r \text{ or } j=j_{\text{rand}}) \\ x_{j,i,g} & \text{another} \end{cases} \quad (16)$$

The probability of crossover ( $C_r$ ) with a range of 0-1 is the value specified by the users to control the distribution of parameter values duplicated from the mutant.  $\text{rand}_j(0,1)$  is a random value that determines whether the vector in crossover or not. If the value  $\text{rand}_j(0,1)$  of a vector is less then  $C_r$ , the value of the vector to be duplicated in the trial vector is a mutant vector. If the opposite is true, then the value of the vector to be duplicated in the trial vector is the initial vector [12]–[14].

Next step is the selection. The purpose of this step is to determine the vector that will become members of the population for the next iteration. If the trial vector ( $u_{i,g}$ ), has the objective function value equal to or smaller than the target vector ( $x_{i,g}$ ), then he changed the target vector in the generation or the next iteration. Conversely, if the trial vector ( $u_{i,g}$ ) has the objective function value that is greater than the target vector ( $x_{i,g}$ ), the vector targets remain a member of the generation or the next iteration [12]–[14]. This is stated in (17).

$$x_{i,g} = \begin{cases} u_{i,g} & \text{if } f(u_{i,g}) \leq f(x_{i,g}) \\ x_{j,i,g} & \text{another} \end{cases} \quad (17)$$

## IV. RESULT AND DISCUSSIONS

### A. Case Study I

In this case study, a load frequency control (LFC) of two area power system, popularly known as ‘‘Hadi Saadat’’ model was used. This system comprises of an 11-order model equipped with PID controller as governor controller as shown Fig. 10. To analyze the performance of the system, a small disturbance was applied in area 1 by giving 0.01 step input of load. Fig. 11-13 illustrate time domain simulations of inter-area power and frequency oscillation in area 1 and 2. It was observed that due to a small disturbance in area 1, overshoot of power signal in area 1, area 2 and inter-area emerged. It was noticeable that the worst dynamic response, represented as an oscillatory condition of the system was monitored when only the integral controller of the governor was considered.

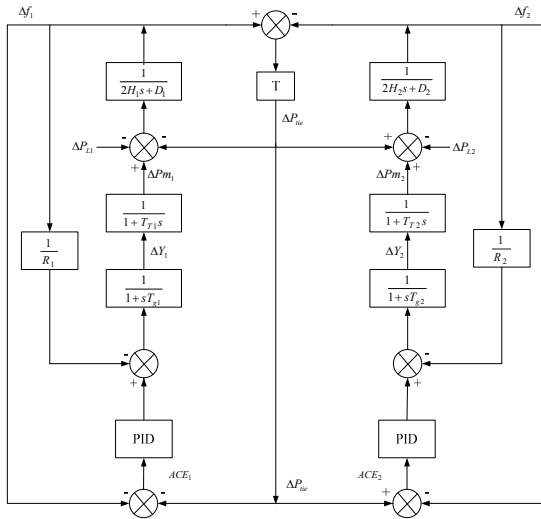


Fig. 10. Frequency oscillation in area 1.

Enhancement of system dynamic response was monitored when the PID controller was applied. Moreover, using the proposed tuning algorithm, the system dynamic response improved more, indicated by lower overshoot and faster settling time. The comparison of overshoot and setting time with three different control approaches are presented in Table I-III.

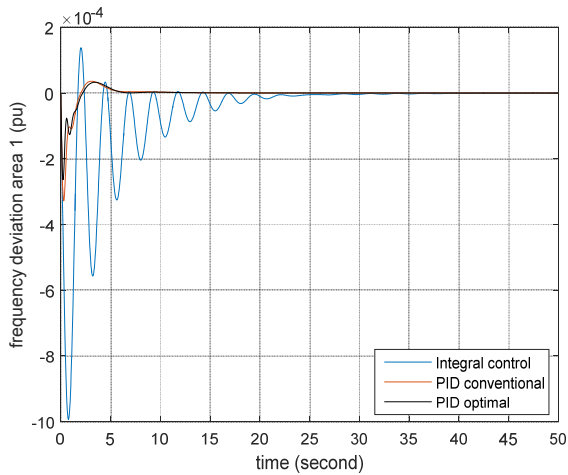


Fig. 11. Frequency oscillation in area 1.

TABLE I  
OVERSHOOT AND SETTLING TIME OF FREQUENCY AREA 1

	Cases		
	Integral Control	PID	PID Optimal
Overshoot	-0.0009936	-0.000328	-0.0002639
Settling time	>20	>5	>5

TABLE II  
OVERSHOOT AND SETTLING TIME OF FREQUENCY AREA 2

	Cases		
	Integral Control	PID	PID Optimal
Overshoot	-0.000285	-0.0000303	-0.00002096
Settling time	>50	>10	>10

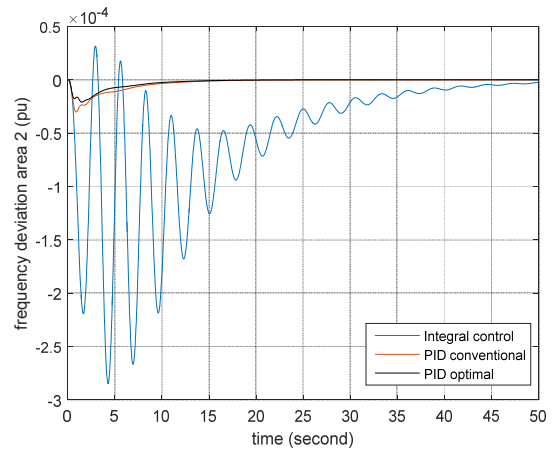


Fig. 12. Frequency oscillation in area 2

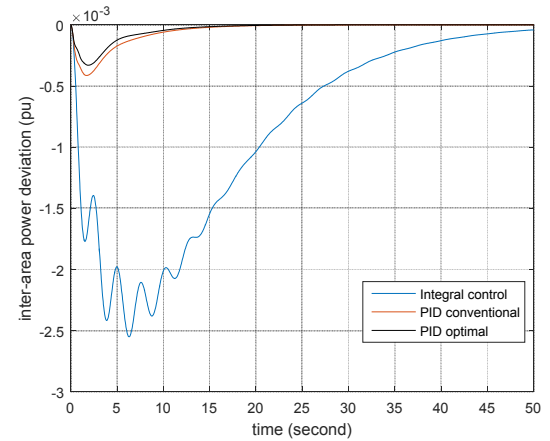


Fig. 13. Inter-area power oscillation.

B. Case Study 2

In the second case study, load frequency control two area power system was considered as a benchmark for the frequency analysis study. A modification was made in the system by putting PV plant in area 1. Moreover, the system comprises a 13-order model equipped with a PID controller as governor controller and PV plant integrating into area 1. To analyze the performance of the system, a small disturbance was applied in area 1 by giving 0.01 step input of PV active power. Figs. 14-16 illustrate time domain simulation of inter-area power and frequency oscillations in area 1 and 2. It was found that due to a small disturbance in area 1, overshoot signal in area 1, area 2 and inter-area were observed. It was noticeable that the oscillatory condition of the system with the integral controller only as governor control method results in the worst condition of system dynamic response.

It was also found that by using PID controller as governor controller, the oscillatory circumstances improved, indicated by lower overshoot and faster setting time. Moreover, the best performance was monitored when the PID controller tuned by the DEA.

The comparison of system dynamic performances using three different control approached are presented in Table IV-VI.

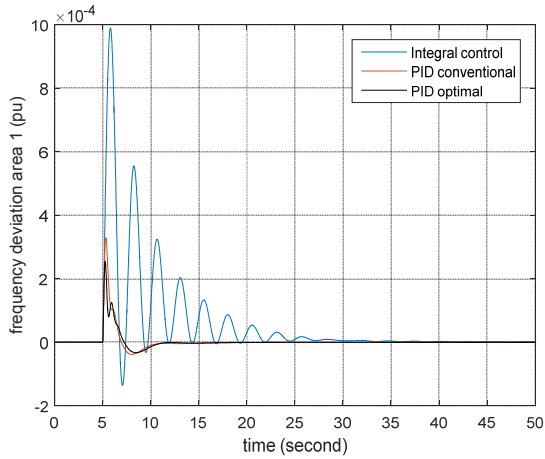


Fig. 14. Frequency oscillation in area 1.

TABLE III  
OVERSHOOT AND SETTLING TIME OF INTER-AREA POWER

	Cases		
	Integral Control	PID	PID Optimal
Overshoot	-0.002548	-0.0004143	-0.0003304
Settling time	>50	>10	>10

TABLE IV  
OVERSHOOT AND SETTLING TIME OF FREQUENCY AREA 1

	Cases		
	Integral Control	PID	PID Optimal
Overshoot	0.00099	0.0003286	-0.000255
Settling time	>20	>5	>5

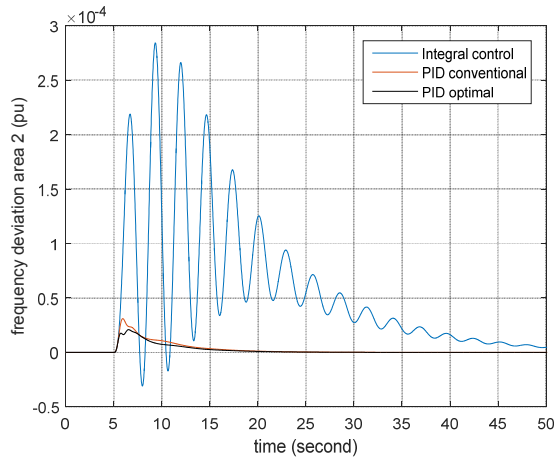


Fig. 15. Frequency oscillation in area 2.

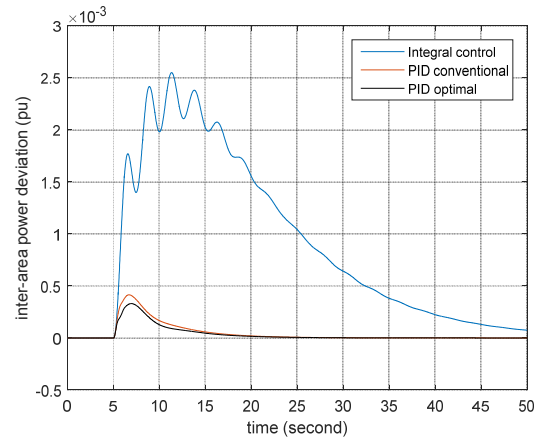


Fig. 16. Inter-area oscillation in area 1

### C. Case Study 3

In the third case study, load frequency control in two area power system was considered as a benchmark for the frequency analysis study. A modification was made to the system by integrating PV plant in area 1. Moreover, the system comprises a 13-order model equipped with a PID controller as governor controller and PV plant integrating into area 1. To analyze the performance of the system, a small perturbation was applied in area 1 by giving 0.01 step input of load changing and PV active power. Figs. 17-19 illustrate time domain simulation of inter-area power and frequency oscillation in area 1 and 2.

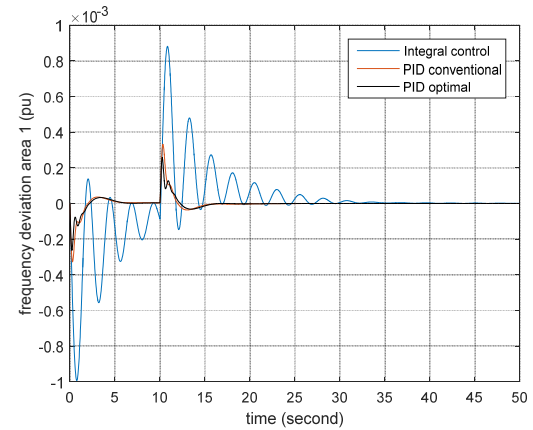


Fig. 17. Inter-area oscillation in area 1.

It was observed that when the system is subjected to a small disturbance in area 1, overshoots of the signal in area 1, area 2 and inter-area power were monitored. Similar to the previous two study cases, the worst system dynamic behavior was monitored when the only integral controller was considered as governor control.

It was also found that implementation of a PID controller as governor controller potentially improve the oscillatory condition of the system. The system dynamic performance can be more enhanced when the PID controller parameters were tuned by DEA.

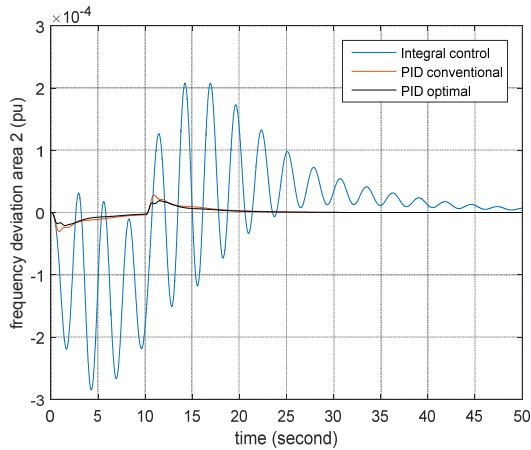


Fig. 18. Inter-area oscillation in area 1.

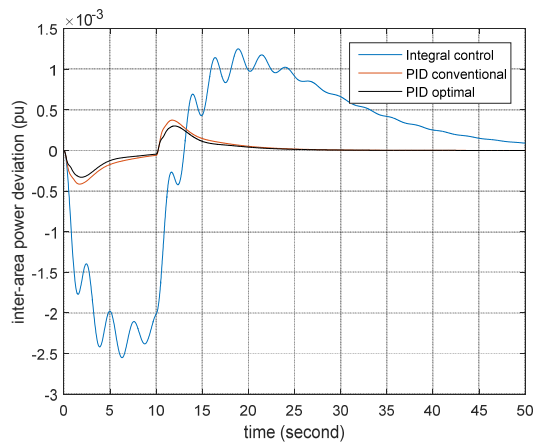


Fig. 19. Inter-area oscillation in area 1.

## V. CONCLUSIONS

Optimization of control parameters of LFC using DEA approach is thoroughly investigated in this work. Three different study cases have been presented to observe the effects of the proposed optimization approach on system dynamic response. It was clearly monitored that by using the DEA procedure, oscillatory conditions when the investigated test system was subjected to small disturbance damped significantly. The system dynamic responses enhanced remarkably, indicated by lower overshoot and faster settling time. It was also monitored that the proposed optimization method can provide an enhancement of system dynamic performance with the high PV penetration level, facilitating the integration of more renewable energy in the power system environment.

## REFERENCES

[1] Y. Tang, J. Yang, and J. Yan, "Intelligent load frequency controller using GrADP for island smart grid with electric vehicles and renewable resources," *Neurocomputing*, vol. 170, pp. 406–416, Dec. 2015.

- [2] R. Farhangi, M. Boroushaki, and S. H. Hosseini, "Load–frequency control of interconnected power system using an emotional learning-based intelligent controller," *Int. J. Electr. Power Energy Syst.*, vol. 36, no. 1, pp. 76–83, Mar. 2012.
- [3] Y. Chabane and A. Ladjici, "Differential evolution for optimal tuning of power system stabilizers to improve power systems small signal stability," in *2016 5th International Conference on Systems and Control (ICSC)*, 2016, pp. 84–89.
- [4] U. K. Rout, R. K. Sahu, and S. Panda, "Design and analysis of differential evolution algorithm based automatic generation control for an interconnected power system," *Ain Shams Eng. J.*, vol. 4, no. 3, pp. 409–421, 2013.
- [5] R. W. W. Atmaja, S. Herlambang, and I. Robandi, "Optimal Design of PID Controller in Interconnected Load Frequency Control using Hybrid Differential Evolution–Particle Swarm Optimization Algorithm," in *Seminar on Intelligent Technology and Its Applications 2014*, 2014.
- [6] H. Saadat, *Power System Analysis McGraw-Hill Series in Electrical Computer Engineering*.
- [7] R. Shah, N. Mithulananthan, and K. Y. Lee, "Large-scale PV plant with a robust controller considering power oscillation damping," *IEEE Trans. Energy Convers.*, vol. 28, no. 1, pp. 106–116, 2013.
- [8] R. Shah and N. Mithulananthan, "A comparison of the ultracapacitor, BESS and shunt capacitor on oscillation damping of power system with large-scale PV plants," in *Power Engineering Conference (AUPEC), 2011 21st Australasian Universities*, 2011, pp. 1–6.
- [9] H. Bevrani, F. Habibi, P. Babahajyani, M. Watanabe, and Y. Mitani, "Intelligent frequency control in an AC microgrid: Online PSO-based fuzzy tuning approach," *IEEE Trans. Smart Grid*, vol. 3, no. 4, pp. 1935–1944, 2012.
- [10] H. Setiadi, W. K. Kautsar, A. Swandaru, and I. Robandi, "Optimal Tuning PID Controller for Inter Area Using Imperialist Competitive Algorithm (ICA)," in *International Seminar on Applied Technology, Science, and Arts*, 2011.
- [11] D. Lastomo, H. Setiadi, and M. R. Djalal, "Design Controller of Pendulum System using Imperialist Competitive Algorithm," *INTEK J. Penelit.*, vol. 4, no. 1, pp. 53–59, 2017.
- [12] K. Price, R. M. Storn, and J. A. Lampinen, *Differential evolution: a practical approach to global optimization*. Springer Science & Business Media, 2006.
- [13] J. H. Van Sickle, K. Y. Lee, and J. S. Heo, "Differential evolution and its applications to power plant control," in *Intelligent Systems Applications to Power Systems, 2007. ISAP 2007. International Conference on*, 2007, pp. 1–6.
- [14] R. Dong, "Differential evolution versus particle swarm optimization for PID controller design," in *Natural Computation, 2009. ICNC'09. Fifth International Conference on*, 2009, vol. 3, pp. 236–240.

## BIOGRAPHIES



**Awan Uji Krismanto** obtained his B. Sc and M. Sc., in Electrical Engineering, from Brawijaya University and Sepuluh Nopember Institute of Technology (ITS) Surabaya, in 2004 and 2010 respectively. Since 2014, Mr. Awan is pursuing Ph.D. program in Electrical Engineering, The University of Queensland, Brisbane, Queensland, Australia. Mr. Awan is a full-time lecturer in the Department of Electrical Engineering, National Institute of Technology, Malang, Indonesia. His research interests include microgrid, smart grid, power system stability, distributed generation, power electronics, and power quality.

**Herlambang Setiadi** received his B. Eng in Electrical Engineering from Sepuluh Nopember Institute of Technology (ITS), Surabaya, Indonesia in 2014 and his M. Sc. in Electrical Power and Control Engineering from Liverpool John Moores University in 2015. Currently, he is pursuing Ph.D. program in Power and Energy System (PES) group, The University of Queensland under Endowment Fund Education Scholarship (LPDP) from Indonesia Government. His research interest includes small signal stability in power systems, renewable energy integration, battery energy storage systems, power system stabilizer, and metaheuristic algorithm.